

Supramolecular Assembly of Aminoethylene-Lipopeptide PMO Conjugates into RNA Splice-Switching Nanomicelles

Jasmin Kuhn, Philipp M. Klein, Nader Al Danaf, Joel Z. Nordin, Sören Reinhard, Dominik M. Loy, Miriam Höhn, Samir El Andaloussi, Don C. Lamb, Ernst Wagner, Yoshitsugu Aoki, Taavi Lehto, and Ulrich Lächelt*

Phosphorodiamidate morpholino oligomers (PMOs) are oligonucleotide analogs that can be used for therapeutic modulation of pre-mRNA splicing. Similar to other classes of nucleic acid-based therapeutics, PMOs require delivery systems for efficient transport to the intracellular target sites. Here, artificial peptides based on the oligo(ethylenamino) acid succinyl-tetraethylenpentamine (Stp), hydrophobic modifications, and an azide group are presented, which are used for strain-promoted azide-alkyne cycloaddition conjugation with splice-switching PMOs. By systematically varying the lead structure and formulation, it is determined that the type of contained fatty acid and supramolecular assembly have a critical impact on the delivery efficacy. A compound containing linolenic acid with three cis double bonds exhibits the highest splice-switching activity and significantly increases functional protein expression in pLuc/705 reporter cells in vitro and after local administration in vivo. Structural and mechanistic studies reveal that the lipopeptide PMO conjugates form nanoparticles, which accelerate cellular uptake and that the content of unsaturated fatty acids enhances endosomal escape. In an in vitro Duchenne muscular dystrophy exon skipping model using H2K-*mdx52* dystrophic skeletal myotubes, the highly potent PMO conjugates mediate significant splice-switching at very low nanomolar concentrations. The presented aminoethylene-lipopeptides are thus a promising platform for the generation of PMO-therapeutics with a favorable activity/toxicity profile.

1. Introduction

Antisense oligonucleotides (ASOs) are a versatile molecular tool to modulate cellular processes by interacting with endogenous nucleic acids. Phosphorodiamidate morpholino oligomers (PMOs) are a class of artificial, uncharged ASOs with favorable stability, nuclease-resistance, low immunogenicity, and toxicity.^[1] A promising therapeutic approach based on ASOs is the modulation of gene expression by interfering with pre-mRNA splicing.^[2] Such splice-switching oligonucleotides (SSOs) represent innovative therapeutics and could be applied for a diverse range of acquired or inherited diseases,^[3] including neuromuscular disorders,^[4] thalassemia,^[5] inflammation,^[6] retinopathies,^[7] and cancer.^[8]

Eteplirsen, a PMO for treatment of Duchenne muscular dystrophy (DMD) and nusinersen, a phosphorothioate oligonucleotide against spinal muscular atrophy (SMA), are first examples of approved SSO therapeutics.^[9] Similar to other therapeutic nucleic acid approaches, SSOs require delivery systems for efficient transport to their target

J. Kuhn, Dr. P. M. Klein, Dr. S. Reinhard, D. M. Loy, M. Höhn, Prof. E. Wagner, Dr. U. Lächelt
Department of Pharmacy and Center for NanoScience (CeNS)
LMU Munich
81377 Munich, Germany
E-mail: ulrich.laechelt@lmu.de
N. Al Danaf, Prof. D. C. Lamb
Department of Chemistry and Center for NanoScience (CeNS)
LMU Munich
81377 Munich, Germany

 The ORCID identification number(s) for the author(s) of this article can be found under <https://doi.org/10.1002/adfm.201906432>.

© 2019 The Authors. Published by WILEY-VCH Verlag GmbH & Co. KGaA, Weinheim. This is an open access article under the terms of the Creative Commons Attribution License, which permits use, distribution and reproduction in any medium, provided the original work is properly cited.

DOI: 10.1002/adfm.201906432

Dr. J. Z. Nordin, Dr. S. El Andaloussi, Dr. T. Lehto
Department of Laboratory Medicine
Karolinska Institutet
17177 Stockholm, Sweden
Dr. J. Z. Nordin, Prof. Y. Aoki
Department of Molecular Therapy
National Institute of Neuroscience
National Center of Neurology and Psychiatry (NCNP)
Kodaira 187-8502, Tokyo, Japan
Dr. T. Lehto
Institute of Technology
University of Tartu
50411 Tartu, Estonia

tissues and intracellular target sites.^[10] Previous strategies for improved delivery of PMOs have been based on cell-penetrating peptides (CPPs),^[11] guanidine dendrimers,^[12] or cationic backbone modifications.^[13] Wood and co-workers have developed highly potent and well-studied PMO conjugates based on arginine-rich CPPs termed Pips that display remarkable efficacy in DMD and SMA mouse models.^[14]

Although not yet conclusively resolved, for the efficient cellular uptake of guanidinium-containing scaffolds, such as arginine-rich CPPs or dendrimers, contribution of nonendocytotic translocation mechanisms is discussed.^[15] A well-established alternative chemical motif of intracellular delivery systems is based on repeated aminoethylene units, such as in polyethylenimine or related polyamines and conjugates.^[16] Although the exact mechanism also here is still disputed, the high efficiency is generally attributed to a characteristic protonation of the repeating aminoethylene units in the endosomal range between pH 5 and 7.4 after endocytotic internalization.^[17] Sequence-defined oligo(ethylenamino) amides based on artificial oligoamino acids and solid-phase synthesis have been established as a delivery platform for charged nucleic acids and other therapeutics, which combines the advantages of aminoethylene based polymers with the chemical precision and versatility of peptides.^[18] Here, the synthetic strategy was utilized for the specific development of new aminoethylene-based PMO conjugates.

2. Results and Discussion

2.1. Conjugate Design and Evaluation

Since PMOs are uncharged nucleic acid analogs, they are not prone to the formation of ionic complexes with positively charged transfecting reagents. Strain-promoted azide-alkyne cycloaddition, initially established by Bertozzi and co-workers,^[19] was used for the covalent linkage of dibenzocyclooctyne (DBCO)-modified PMO and azide-containing artificial peptides. For activity screenings and structural optimizations, a PMO sequence against a thalassemic β -globin intron mutation IVS2-705 was selected to enable quantitative evaluation of splicing correction in different cell lines containing the pLuc/705 construct developed by Ryszard Kole's lab in the 1990s. The cells contain a luciferase reporter, which is interrupted by the globin IVS2-705 resulting in increased luciferase activity depending on successful splice-switching (Figure S1, Supporting Information).^[20] Since the construct exhibits a certain background luciferase activity, luminescence levels were always normalized to the background of untreated cells and expressed as "fold increase in luminescence."

2.2. Lead Identification

To assess the general potential of oligo(ethylenamino) amides for PMO delivery, a first library screen was conducted with a statistical azide-functionalization approach (Figure S2, Supporting Information). Selected representatives of cationic polymers (PAMAM dendrimer G5, PPI dendrimer G3, LPEI 22 kDa) and artificial peptides with different architectures (branched 3-arm,^[21] 4-arm,^[17d,22]

comb-like,^[23] PEGylated,^[24] and lipid-modified^{[25])} were first functionalized with 1.5 eq. of azidobutyric acid NHS ester, subsequently click-conjugated to PMO-DBCO and finally used for transfection of HeLa pLuc/705 cells (Figure S3, Supporting Information). Here, the lipopeptide (LP) #991 was identified as the most efficient facilitator of PMO-mediated splice-switching. It contains the oligo(ethylenamino) acid succinyl-tetraethylene pentamine (Stp) as a cationic building unit, cholanolic acid as a hydrophobic modification and tyrosine, which previously showed beneficial effects on charged nucleic acid delivery.^[25,26] For further validation of this screening hit, a #991 analog with azide-group at a defined position, oligomer #1106 (LP Chola),^[27] was used for transfections in comparison to unmodified #991 and at different PMO to oligomer ratios (Figure 1). Here, 1:1 represents the ratio of PMO to LP in the reaction resulting in an equimolar mixture of PMO-DBCO + LP Chola (noncovalent, #991) or the PMO-LP Chola conjugate (covalent, #1106). Surprisingly, noncovalent PMO formulations with #991 were also able to mediate

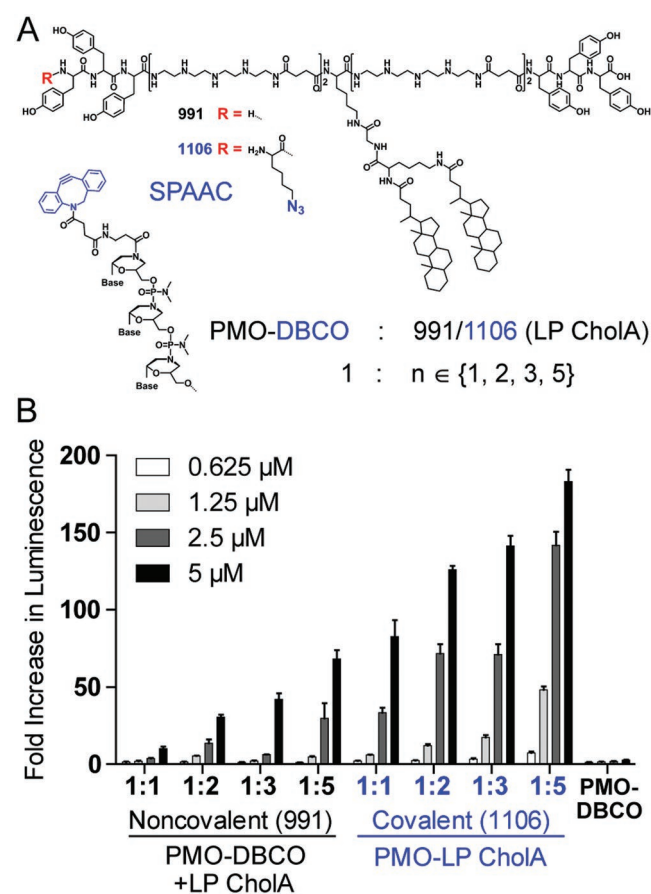


Figure 1. PMO-LP conjugation and evaluation. A) The chemical structure of the lipopeptide #991 and its analog #1106 with *N*-terminal azidobutyric acid for conjugation to PMO-DBCO via strain-promoted azide-alkyne cycloaddition (SPAAC). B) The increase in luminescence in HeLa pLuc/705 cells 24 h after transfection with noncovalent #991 or covalent #1106 formulations at different PMO-DBCO to oligomer ratios. The fold increase in luminescence represents arbitrary light units normalized to the mean background level of buffer treated cells. Data are presented as mean \pm SD ($n = 3$). Additional cell viability data (MTT) are provided in Figure S4 of the Supporting Information.

increased luciferase activity, but only at higher oligomer to PMO ratios. Covalent formulations (PMO-LP CholA) were superior in all cases, but also here a beneficial effect of additional unconjugated LP was evident. To validate the formulation via click reaction, HeLa pLuc/705 cells were treated side by side with the PMO-LP CholA 1:1 formulation and the purified PMO-LP CholA conjugate (Figure S5, Supporting Information). Both PMO formulations mediated comparable levels of luciferase activity, which confirms the reliability of the formulation approach.

2.3. Structural Variations

First, the impact of the repeated aminoethylene motif in the identified lipopeptide architecture was assessed in systematic variations of the lead structure #1106 by replacement of the contained oligoamino acid Stp with basic α -amino acids lysine, arginine, histidine, their combinations, or a 6-aminohexanoic acid-arginine motif (RXR).^[11c,d] Although the derivatives were designed to contain an equal number of protonatable amines in the biologically relevant pH range above pH 5, the substitution of Stp resulted in a complete loss of activity (Figure S6, Supporting Information). This indicates that the artificial oligoamino acid Stp is an essential part of this particular lipopeptide architecture, presumably due the unique endosomal protonation characteristics of repeated aminoethylene motifs. By contrast, substitution of unsaturated fatty acids for the cholanic acid part resulted in improved activity (Figure S7, Supporting Information). This is in line with previous findings that the hydrophobic core of Pip6a derivatives is a critical element for efficient PMO delivery.^[14a] Based on this observation, a series of #1106 analogs containing fatty acids with different numbers of unsaturated bonds was synthesized and functional luciferase expression was assessed in a kinetic study 12 to 72 h after transfection (Figure 2). Here, a distinct dependence of splice-switching activity on the contained fatty acids and the degree of unsaturation was observed: the luminescence increases gradually with increasing number of unsaturated bonds up to three

(Figure 2B, left, top). The PMO conjugate containing linolenic acid with three double bonds (PMO-LP LenA) promoted the highest splice-switching at 5×10^{-6} M concentration. The high activity of PMO-LP LenA was not exceeded by conjugates containing fatty acids with four to six double bonds (Figure 2B, left, bottom). In addition to HeLa, three other cell lines were treated with the same set of PMO conjugates to confirm the general ability to mediate splice-switching of thalassemic β -globin IVS2-705 (Figure S10, Supporting Information). Similar structure–activity relationships and significant splice-switching activities were also observed in pLuc/705 based human hepatoma (Huh7), murine neuroblastoma (Neuro2A), and murine myoblast (C2C12) cells.^[28]

The PMO-sequence specificity was assessed in HeLa pLuc/705 treatments with PMO-LP LenA 1:1 and 1:3 formulations containing either PMO IVS2-705 or 51D (Figure S11, Supporting Information). The data illustrate a high increase in luminescence mediated by the specific PMO-705 in contrast to a very low unspecific response toward the PMO-51D formulations.

In all transfections the activities of PMO-LP conjugates showed a strong dose-dependency. Upon decreasing the concentration of PMOs to 0.625×10^{-6} M, the activity and increase in luminescence dropped to low levels (Figure 2B, middle). As observed before (Figure 1B), additional unconjugated peptide enhanced the splice-switching activity and a high increase in luminescence was achieved by the PMO-LP 1:3 formulations at low PMO concentrations (Figure 2B, right, Figure S8, Supporting Information).

A systematic dose titration clearly illustrated the shifted splice-switching activities of PMO-LP LenA at 1:1 or 1:3 ratio on the RNA and protein activity level (Figure 3). The ratio between aberrant and corrected splicing was determined by RT-PCR specific for a sequence surrounding the β -globin IVS2 (Figure 3A). The band intensities of related PCR products (268 bp aberrant, 142 bp corrected) indicate that complete splicing-correction was achieved with PMO-LP LenA 1:3 at a concentration of 1.25×10^{-6} M PMO whereas, at a 1:1 ratio, 2.5×10^{-6} M PMO were required. This also correlates with the dose-response at the luciferase activity level (Figure 3B). Bare PMO-DBCO, up

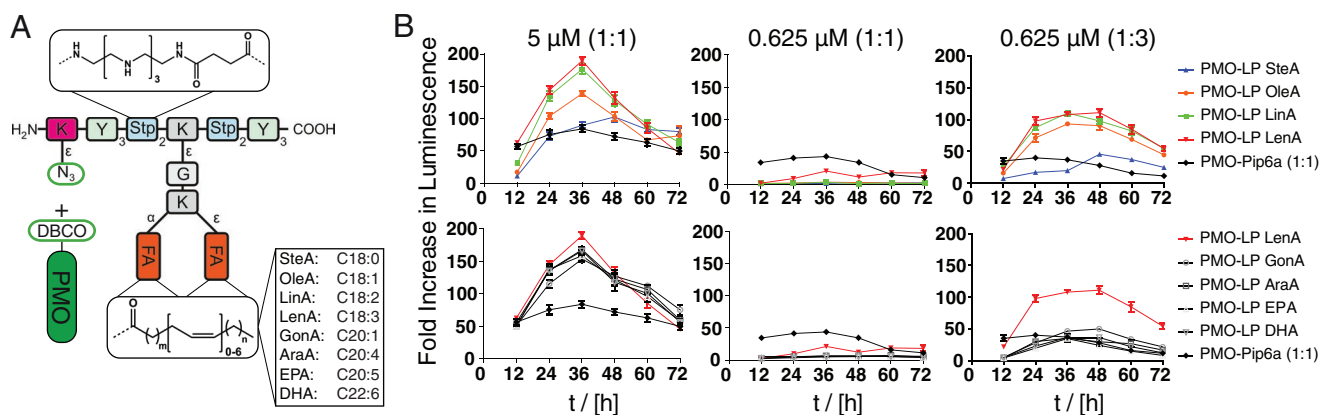


Figure 2. Structure–activity and formulation–activity relationships of PMO-LP conjugates. A) A schematic illustration of artificial lipopeptides (LPs) with systematic variation of contained fatty acids (FA) with 0 (stearic acid, SteA, C18:0) to 6 (docosahexaenoic acid, DHA, C22:6) all-cis double bonds. B) Kinetics of the increase in luminescence between 12 to 72 h after transfection with PMO conjugate formulations at 1:1 (left, middle) or 1:3 (right) PMO-DBCO to LP ratio. Fold increase in luminescence represents arbitrary light units normalized to the mean background levels of buffer treated cells. Figures show a comparison between LPs containing 0 to 3 (top) or 3 to 6 cis double bonds (bottom). A Pip6a-azide derivative served as a positive control in the same PMO-DBCO conjugation protocol at a 1:1 ratio. Data are presented as mean \pm SD ($n = 3$). A complete set of PMO formulations at different concentrations are provided in Figures S8 and S9 of the Supporting Information.

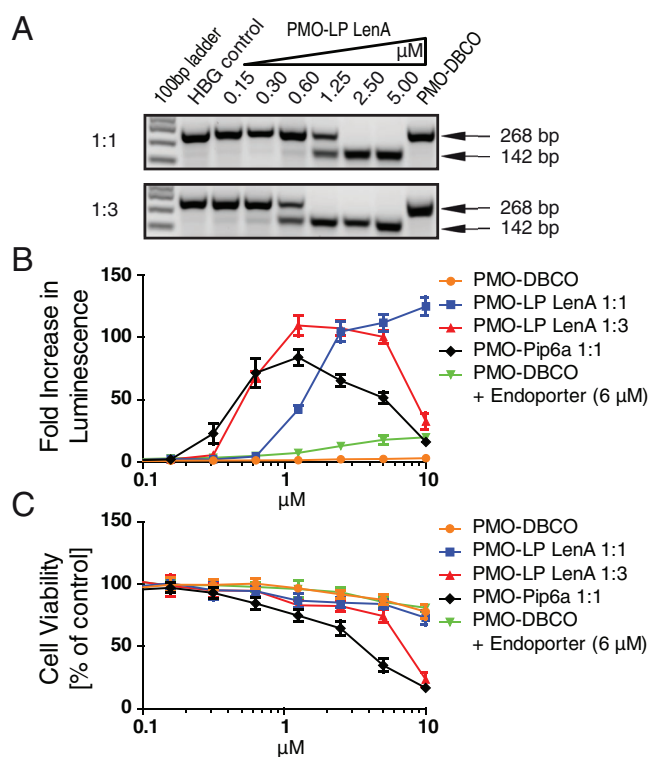


Figure 3. Dose–response effects of PMO formulations on HeLa pLuc/705 cells. A) Detection of corrected β -globin intron splicing by RT-PCR. The total RNA was extracted from cells 24 h after PMO-LP LenA 1:1 (top) or 1:3 (bottom) treatment and amplified using RT-PCR specific for a sequence surrounding β -globin IVS2. Arrows indicate the PCR products resulting from unchanged aberrant (268 bp) and corrected (142 bp) mRNA splicing. PMO-DBCO was used at 5×10^{-6} M concentration. B) Fold increase in luminescence and C) metabolic activity 24 h after treatment with PMO-DBCO formulations containing 0.156 to 10×10^{-6} M PMO. Free PMO-DBCO, PMO-DBCO formulations with constant 6×10^{-6} M “Endo-Porter” reagent (Gene Tools, LLC) and PMO-Pip6a served as references. Data are presented as mean \pm SD ($n = 3$).

to a concentration of 10×10^{-6} M, was not able to increase luciferase activity significantly. Dose titrations of both PMO-LP LenA 1:1 and 1:3 formulations side by side revealed equal maximum levels between 2.5 and 5×10^{-6} M and an enhanced potency for the 1:3 formulation at lower concentrations due to the additional fraction of free LP. At the high concentration of 10×10^{-6} M, the excess of unconjugated LP (20×10^{-6} M) also mediated cytotoxicity (Figure 3C), which was responsible for the drop of luciferase activity. An azide-containing derivative of the efficient CPP Pip6a served as a positive control and benchmark compound; the PMO-DBCO conjugation was carried out analog to the LP formulations at a 1:1 ratio. In direct comparison to Pip6a-PMO, PMO-LP LenA 1:3 showed a comparable potency at low concentrations, higher maximal luciferase activity, and reduced cytotoxicity at higher concentrations. PMO-LP LenA 1:1 exhibited the best tolerability and no observable signs of cytotoxicity or reduced luciferase activity up to a concentration of 10×10^{-6} M PMO. Notably, all formulations clearly outperformed the commercial noncovalent PMO delivery reagent “Endo-Porter,” which was supplemented at constant 6×10^{-6} M concentration, as recommended by the distributor.^[12,29]

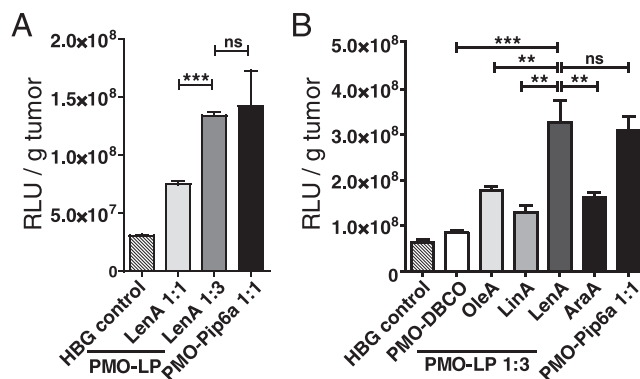


Figure 4. Ex vivo luciferase activity in subcutaneous HeLa pLuc/705 tumors 48 h after local injection. A) Comparison of PMO-LP LenA formulations at a 1:1 or 1:3 ratio. B) Comparison of PMO-LP (1:3) formulations with fatty acids containing 1 (OleA), 2 (LinA), 3 (LenA) or 4 (AraA) double bonds. A Pip6a-azide derivative served as a positive control in the same PMO-DBCO conjugation protocol at a 1:1 ratio. All formulations contained 450 μ g PMO. Data are presented as mean \pm SD ($n = 3$).

Next, to understand if these structure–activity relationships identified under cell culture conditions would also translate to a more complex in vivo environment, PMO-LP formulations were locally injected into subcutaneous HeLa pLuc/705 xenograft tumors in mice (Figure 4). The quantification of ex vivo luciferase activity in the tumor confirmed the two key findings of the previous in vitro studies: first, the fraction of free peptide in PMO-LP 1:3 formulations enhances splice-switching activity (Figure 4A), and second, LP LenA containing linolenic acid with three unsaturated bonds is superior to analogs containing fatty acids with one (OleA), two (LinA), or four (AraA) double bonds (Figure 4B). The studies demonstrate that PMO-LP LenA 1:3 represents a potent formulation with significant splice switching activity in the investigated models.

The exclusive investigation of luminescence levels as final result of a complex transfection process is not sufficient to elucidate the underlying mechanisms. Therefore, specific mechanistic studies were conducted to clarify the impact of free LP (Figure 5) and unsaturated fatty acids (Figure 6) in the PMO-LPs.

2.4. Particle Formation

To investigate the formation of PMO-LP nanoparticles, fluorescence correlation spectroscopy (FCS) experiments with PMO-LP LenA 1:1 and 1:3 formulations at various PMO-LP concentrations each containing 50×10^{-9} M Alexa Fluor 647 labeled PMO (AF647-PMO) were carried out (Figure 5A). FCS is based on the diffusion of fluorescent molecules through a small confocal volume (≈ 1 fL), where the fluorescence signal is recorded and the fluctuations analyzed.^[30] Changes in the rate of diffusion due to the assembly of PMO-LP nanoparticles causes a shift in the temporal autocorrelation function (ACF) of the FCS signal to slower timescales. Already at 1.25×10^{-6} M PMO, a significantly slower ACF decay of the PMO-LP 1:3 formulation was observed, which did not significantly change at higher concentrations. Although, a decrease in the decay time of the ACF of the PMO-LP 1:1 formulation was observed at a concentration of 2.5×10^{-6} M, it was

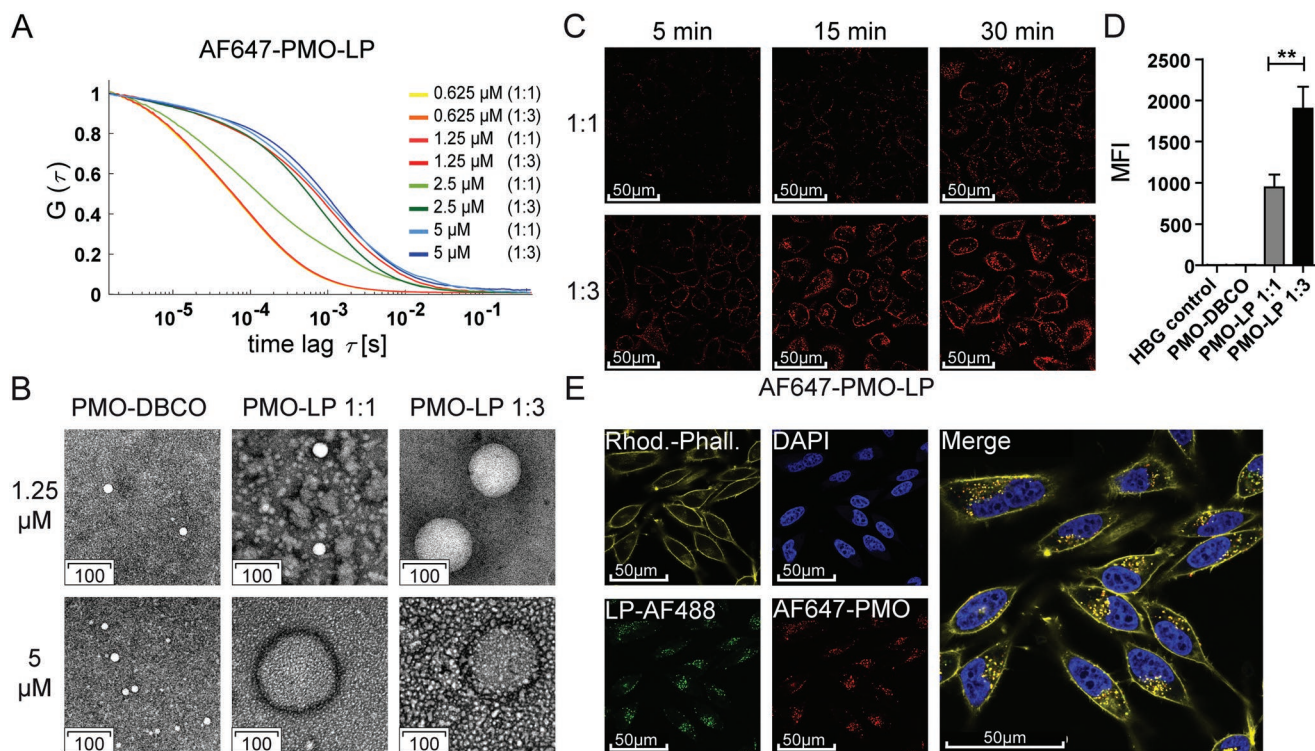


Figure 5. Impact of free LP in the PMO formulations. A) Fluorescence correlation spectroscopy (FCS) measurements of PMO-LP LenA 1:1 and 1:3 formulations at different concentrations where 50×10^{-9} M of Alexa Fluor 647 labeled PMO-DBCO (AF647-PMO) was included. The slower decay of the autocorrelation function represented by a shift toward higher time lag τ indicates the slower diffusion of AF647-PMO-LP nanoparticles. B) Transmission electron microscopy (TEM) images of bare PMO-DBCO or formulations with LP LenA at 1:1 and 1:3 ratio. C) Confocal laser scanning microscopy (CLSM) images of HeLa pLuc/705 cells 5, 15, or 30 min after transfection with PMO-LP LenA 1:1 or 1:3 (0.625×10^{-6} M PMO) containing 20% AF647-PMO. D) The uptake of PMO-LP LenA 1:1 and 1:3 (0.625×10^{-6} M PMO) containing 5% AF647-PMO into HeLa pLuc/705 cells 15 min after transfection determined by flow cytometry (median fluorescence intensity, MFI, $n = 3$) is shown. E) CLSM images of HeLa pLuc/705 cells 24 h after transfection with PMO-LP LenA 1:3 containing 20% AF647-PMO and 20% Alexa Fluor 488-labeled free LP-LenA (LP-AF488). Nuclei were stained with DAPI (blue), actin filaments with rhodamine phalloidin (yellow). The merged channel indicates colocalization (yellow) of AF647-PMO-LP and free LP-AF488. Additional FCS, TEM, CLSM, and flow cytometry data are provided in Figures S12–S21 of the Supporting Information.

only at a concentration of 5×10^{-6} M that the decay time of the ACF approached that of the 1.25×10^{-6} M of the 1:3 formulation.

These observations indicate a dose-dependent self-association and complex formation of PMO-LP formulations. In this process, the fraction of free LP in 1:3 formulations seems to contribute to the complex assembly at low PMO concentrations. Interestingly, neither labeled PMO-DBCO (at 1×10^{-6} and 50×10^{-6} M concentrations, Figure S12, Supporting Information) nor LP LenA alone (below 10×10^{-6} M concentrations, Figures S13 and S14, Supporting Information) showed substantial supramolecular assembly, compared to the PMO-LP LenA formulations. The conjugation seems to change the assembly tendency compared to the unconjugated reaction partners. Similar findings were obtained by transmission electron microscopy (TEM, Figure 5B). At a PMO concentration of 5×10^{-6} M, spherical nanomicelles were detected in both PMO-LP 1:1 and 1:3 formulations, whereas, at 1.25×10^{-6} M PMO, similar complexes could only be observed in the 1:3 formulation. Free PMO-DBCO did not form particles at any concentration. To address the impact of unconjugated LP on the PMO transfection process, cellular uptake of PMO-LP 1:1 and 1:3 was investigated by confocal laser scanning microscopy (CLSM, Figure 5C) and flow cytometry (Figure 5D). Already

5 min after addition of the formulations to HeLa pLuc/705 cells, cellular association could be observed in the 1:3 formulation, which rapidly increased over time. Despite the same PMO concentration, cellular uptake was significantly enhanced 15 min after transfection by the fraction of free peptide in the 1:3 formulation compared to 1:1 (Figure 5D), which presumably is a result of the facilitated complex formation and nanoparticle internalization.^[31] The resulting higher PMO uptake after 24 h (Figure S21, Supporting Information) is in line with the enhanced splice-switching activity mediated by PMO-LP 1:3 formulations. The intracellular fate of PMO-LP and free LP was assessed in an additional CLSM experiment with a PMO-LP LenA 1:3 formulation containing AF647-PMO and Alexa Fluor 488 labeled free LP LenA (Figure 5E). The images verify that both separate components co-localize within the cells and seem to remain associated up to 24 h after transfection.

2.5. Membrane Interaction

From additional flow cytometry studies, it is evident that the beneficial effect of the unconjugated LP in 1:3 formulations on the cellular uptake is independent of the different lipid or

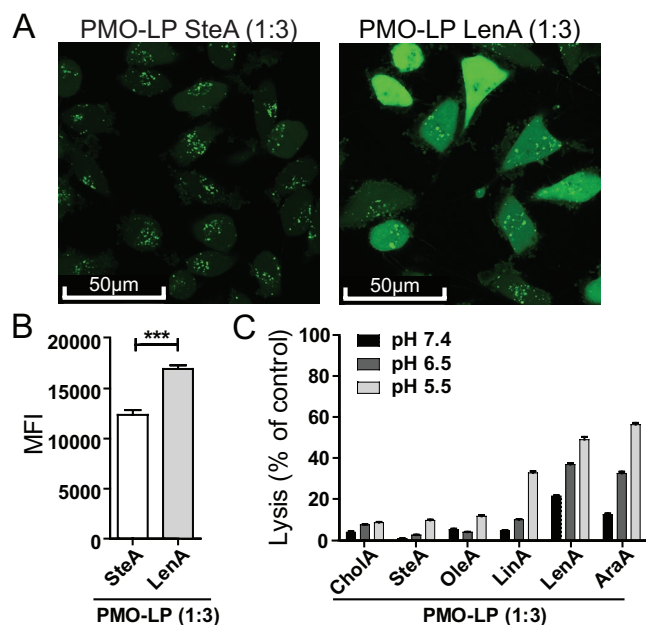


Figure 6. Impact of unsaturated fatty acids on cellular membrane interactions. A) CLSM images of HeLa pLuc/705 cells treated with 0.45 mg mL^{-1} calcein and $5 \times 10^{-6} \text{ M}$ PMO-LP SteA (1:3) or PMO-LP LenA (1:3) for 4 h. B) The cellular calcein fluorescence intensity determined by flow cytometry (median fluorescence intensity, MFI, $n = 3$) is shown. C) Hemoglobin release was determined photometrically for 3.75×10^6 erythrocytes that were incubated for 60 min with $2.5 \times 10^{-6} \text{ M}$ PMO-LP (1:3) at pH 7.4, 6.5 and 5.5. Values were normalized to positive control samples treated with 1% Triton X-100 (100% lysis). Data are presented as mean \pm SD ($n = 4$).

fatty acid modifications (Figure S21, Supporting Information). 1:1 formulations with LP containing cholanic acid or fatty acids with 1 to 4 unsaturated bonds mediated comparable levels of cellular PMO uptake. In all cases, a distinct PMO uptake enhancement was observed in the corresponding 1:3 formulations. Obviously, enhanced cellular uptake can explain the advantage of free LP in the formulations, but not the advantage of a specific fatty acid content. Therefore, the high efficacy of LP LenA must be the result of a different mechanism associated with the intracellular PMO trafficking. The lipid modifications turn the cationic conjugates into amphiphilic structures and provide the potential for membrane interactions. It has been shown previously that unsaturated fatty acids can mediate pH-dependent membrane lytic activity in nucleic acid transfecting agents.^[18b,32] For this reason, we hypothesize membrane interaction and endosomal release after endocytotic internalization as being a potential explanation for the superiority of PMO-LP LenA. An endosomal membrane integrity and release assay^[17d,33] was carried out with fluorescent calcein being loaded into endosomes during transfection with PMO-LP SteA (saturated) or PMO-LP LenA (unsaturated) formulations (Figure 6A). In both cases, calcein was taken up efficiently (Figure 6B) but it was only in the case of PMO-LP LenA that a broad and homogenous distribution of fluorescence intensity were evident over the cell indicating release of the fluid phase marker calcein from the endosomes. An erythrocyte leakage assay verified the pH-dependent membrane interactive potential of PMO-LP containing unsaturated fatty acids

(Figure 6C). The set of PMO-LP formulations containing CholA or fatty acids with zero to four double bonds was incubated with erythrocytes at physiological pH 7.4 or endolysosomal pH 6.5 and 5.5. A clear trend showed an increasing erythrocyte leakage, particularly at acidic pH, with an increasing number of double bonds. The highest lytic activity was observed with PMO-LP LenA and AraA, which altogether supports the initial hypothesis of increased endosomal membrane interaction and release of the PMO-LP formulation containing unsaturated bonds. Additional erythrocyte leakage assays were conducted to clarify the contribution of free LP in PMO-LP 1:3 formulations (1 eq. PMO-LP conjugate, 2 eq. free LP) on membrane disruption (Figure S22, Supporting Information). Erythrocytes were treated with free LP SteA or LenA ($2.5, 5, 7.5 \times 10^{-6} \text{ M}$), PMO-LP SteA or LenA 1:1 ($2.5, 7.5 \times 10^{-6} \text{ M}$) and PMO-LP SteA or LenA 1:3 ($2.5 \times 10^{-6} \text{ M}$) formulations. The concentrations were chosen to enable direct comparison of equal free and total LP contents. Here, several significant observations were made. First, the higher lytic activity of LP LenA compared to LP SteA was confirmed in all three different states: free LP, PMO-LP 1:1 and 1:3 formulations. Second, free LP mediated by far the highest erythrocyte leakage in all cases which indicates a reduction of lytic potential due to conjugation. Third, PMO-LP 1:3 ($2.5 \times 10^{-6} \text{ M}$) exhibited lower lytic activity than the corresponding samples with equal amount of free ($5 \times 10^{-6} \text{ M}$) or total ($7.5 \times 10^{-6} \text{ M}$) LP content. Apparently, the presence of PMO-LP reduces lytic potential of free LP which can be explained by the observed coassembly into nanomicelles. Finally, the initially speculated contribution of free LP on membrane disruption was confirmed: in both cases (LP SteA, LP LenA), PMO-LP 1:3 formulations mediated higher lytic activity than the corresponding 1:1 formulations.

2.6. DMD Myotube Treatment

As an additional model with clinical relevance, an alternative PMO sequence 51D^[34] mediating exon skipping in H2K-*mdx52* dystrophic skeletal myotubes was selected (Figure 7). In *mdx52* mice, a deletion of dystrophin exon 52 was generated by gene targeting,^[35] which belongs to the “deletion mutation hotspot”^[36] of human DMD. H2K-*mdx52* myotubes were treated with varying concentrations of PMO-LP LenA 1:1 at $(12.5\text{--}50) \times 10^{-9} \text{ M}$ or 1:3 at $(2\text{--}50) \times 10^{-9} \text{ M}$ and Pip6a at $50 \times 10^{-9} \text{ M}$. After 48 h, the exon skipping rate of extracted RNA was determined by RT-PCR amplification of dystrophin exons 49–54 and microchip electrophoresis. In this in vitro DMD exon skipping model the PMO-LP formulations displayed remarkably high activity. Both the 1:1 and 1:3 formulations achieved >85% exon skipping at a concentration of $50 \times 10^{-9} \text{ M}$. The exon skipping rate mediated by the 1:1 formulation dropped to $\approx 43\%$ at $25 \times 10^{-9} \text{ M}$ and 24% at $12.5 \times 10^{-9} \text{ M}$ concentrations. Consistent with the findings obtained in HeLa pLuc/705 cells, also in H2K-*mdx52* dystrophic myotubes the PMO conjugates strongly benefit from the additional free LP in the formulation. PMO-LP LenA 1:3 mediated significantly higher exon skipping ($\approx 25\%$ at $2 \times 10^{-9} \text{ M}$, $\approx 100\%$ at $50 \times 10^{-9} \text{ M}$) compared to PMO-Pip6a ($\approx 6\%$ at $50 \times 10^{-9} \text{ M}$, $\approx 77\%$ at $400 \times 10^{-9} \text{ M}$, Figure S23, Supporting Information).

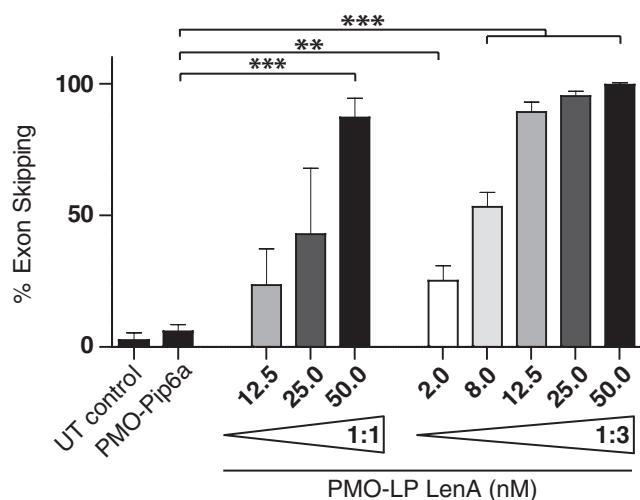


Figure 7. Exon skipping efficiency in H2K-*mdx52* myotubes. H2K-*mdx52* myoblasts were differentiated for 3 days and treated with varying concentrations of PMO-LP LenA 1:1 or 1:3. PMO-Pip6a 1:1 at 50×10^{-9} M concentration and untreated (UT) cells served as controls. After 48 h, the total RNA was extracted from the cells and RT-PCR amplifying cDNA from exons 49–54 was carried out. PCR products were detected using a microchip electrophoresis system. Exon-skipping efficiency (%) was calculated as (exon-skipped transcript molarity)/(unskipped + exon-skipped transcript molarity) \times 100%. Data are presented as mean \pm SD ($n = 3$). Additional data of PMO-LP LenA 1:1 and PMO-Pip6a are provided in Figure S23 of the Supporting Information.

3. Conclusion

In summary, we report novel aminoethylene lipopeptide-PMO conjugates with a high potential for promoting splice-switching PMO delivery. During the screening and optimization process, two key parameters of highly active formulations were identified: (1) PMO-LP conjugates containing linolenic acid mediate the highest effects, and (2) additional unconjugated LP in the formulation enhances the potency and activity at low concentrations. The PMO-LP conjugates self-associate into nanocomplexes in a concentration-dependent fashion and a fraction of additional free LP in the formulation contributes to the particle formation. The content of unsaturated fatty acid LenA was found to facilitate endosomal release after cellular internalization, most likely via membrane interactions. The splice-switching activity of the PMO-LP formulations was confirmed in human cervix carcinoma (HeLa), human hepatoma (Huh7), murine neuroblastoma (Neuro2A), and murine myoblast (C2C12) pLuc/705 cells in vitro as well as after local injection into HeLa pLuc/705 tumors in vivo. The encouraging splice-switching activity was additionally confirmed in H2K-*mdx52* dystrophic skeletal muscle cells where the identified PMO-LP formulation exhibited remarkably high potency and mediated significant exon skipping at low concentration $<10 \times 10^{-9}$ M. The presented LP conjugates and formulations are considered a highly potent platform for the delivery of PMO therapeutics with antisense or splicing-modifying mechanism.

Supporting Information

Supporting Information is available from the Wiley Online Library or from the author.

Acknowledgements

The authors thank Olga Brück and Wolfgang Rödl for technical assistance, Susanne Kempter for support during TEM measurements, and Tobias Burghardt for assistance in the chemistry lab. The authors are grateful for financial support from the Excellence Cluster Nanosystems Initiative Munich (NIM) and the Center for NanoScience Munich (CeNS). Funding through the DFG SFB 1032 (Projects B3 and B4) is greatly appreciated. T.L. was supported by Estonian Research Council (Grant No. PSG226). S.E.A. was supported by the Swedish Medical Research Council (VR-Med) and the Swedish Strategic Science Foundation (SSF-IRC). J.Z.N. was supported by SSMF. U.L. appreciates the support by the Galenus-Privatstiftung (Vienna, Austria).

Conflict of Interest

The authors declare no conflict of interest.

Keywords

antisense, delivery, morpholino, PMO conjugate, splice-switching

Received: August 6, 2019

Revised: August 23, 2019

Published online: September 19, 2019

- [1] J. Summerton, D. Weller, *Antisense Nucleic Acid Drug Dev.* **1997**, *7*, 187.
- [2] a) J. Bauman, N. Jearawiriyapaisarn, R. Kole, *Oligonucleotides* **2009**, *19*, 1; b) R. Kole, A. R. Krainer, S. Altman, *Nat. Rev. Drug Discovery* **2012**, *11*, 125.
- [3] M. A. Havens, M. L. Hastings, *Nucleic Acids Res.* **2016**, *44*, 6549.
- [4] a) M. G. Dunckley, M. Manoharan, P. Villiet, I. C. Eperon, G. Dickson, *Hum. Mol. Genet.* **1998**, *7*, 1083; b) F. Muntoni, M. J. Wood, *Nat. Rev. Drug Discovery* **2011**, *10*, 621; c) J. Alter, F. Lou, A. Rabinowitz, H. Yin, J. Rosenfeld, S. D. Wilton, T. A. Partridge, Q. L. Lu, *Nat. Med.* **2006**, *12*, 175; d) Q. L. Lu, C. J. Mann, F. Lou, G. Bou-Gharios, G. E. Morris, S. A. Xue, S. Fletcher, T. A. Partridge, S. D. Wilton, *Nat. Med.* **2003**, *9*, 1009; e) A. H. M. Burghes, V. L. McGovern, P. N. Porensky, C. Mitrpant, S. D. Wilton, A. K. Bevan, B. K. Kaspar, K. D. Foust, *Hum. Mol. Genet.* **2011**, *21*, 1625.
- [5] a) Z. Dominski, R. Kole, *Proc. Natl. Acad. Sci. USA* **1993**, *90*, 8673; b) S. Svasti, T. Suwanmanee, S. Fucharoen, H. M. Moulton, M. H. Nelson, N. Maeda, O. Smithies, R. Kole, *Proc. Natl. Acad. Sci. USA* **2009**, *106*, 1205.
- [6] M. A. Graziewicz, T. K. Tarrant, B. Buckley, J. Roberts, L. Fulton, H. Hansen, H. Orum, R. Kole, P. Sazani, *Mol. Ther.* **2008**, *16*, 1316.
- [7] a) X. Gérard, I. Perrault, A. Munnich, J. Kaplan, J.-M. Rozet, *Mol. Ther. – Nucleic Acids* **2015**, *4*, e250; b) A. Garanto, D. C. Chung, L. Duijkers, J. C. Corral-Serrano, M. Messchaert, R. Xiao, J. Bennett, L. H. Vandenberghe, R. W. Collin, *Hum. Mol. Genet.* **2016**, *25*, 2552.
- [8] a) F. Zammarchi, E. de Stanchina, E. Bournazou, T. Supakorndej, K. Martires, E. Riedel, A. D. Corben, J. F. Bromberg, L. Cartegni, *Proc. Natl. Acad. Sci. USA* **2011**, *108*, 17779; b) D. R. Mercatante, C. D. Bortner, J. A. Cidlowski, R. Kole, *J. Biol. Chem.* **2001**, *276*, 16411.
- [9] a) Y. Shimizu-Motohashi, H. Komaki, N. Motohashi, S. Takeda, T. Yokota, Y. Aoki, *J. Pers. Med.* **2019**, *9*, 1; b) E. W. Ottesen, *Transl. Neurosci.* **2017**, *8*, 1.
- [10] a) U. Lächelt, E. Wagner, *Chem. Rev.* **2015**, *115*, 11043; b) C. Godfrey, L. R. Desviat, B. Smedsrød, F. Piétri-Rouxel, M. A. Denti, P. Disterer, S. Lorain, G. Nogales-Gadea, V. Sardone, R. Anwar, S. El Andaloussi, T. Lehto, B. Khoo, C. Brolin,

- W. M. C. van Roon-Mom, A. Goyenvalle, A. Aartsma-Rus, V. Arechavala-Gomez, *EMBO Mol. Med.* **2017**, *9*, 545.
- [11] a) H. M. Moulton, M. C. Hase, K. M. Smith, P. L. Iversen, *Anti-sense Nucleic Acid Drug Dev.* **2003**, *13*, 31; b) H. M. Moulton, M. H. Nelson, S. A. Hatlevig, M. T. Reddy, P. L. Iversen, *Bioconjugate Chem.* **2004**, *15*, 290; c) S. Abes, H. M. Moulton, P. Clair, P. Prevot, D. S. Youngblood, R. P. Wu, P. L. Iversen, B. Lebleu, *J. Controlled Release* **2006**, *116*, 304; d) R. P. Wu, D. S. Youngblood, J. N. Hassinger, C. E. Lovejoy, M. H. Nelson, P. L. Iversen, H. M. Moulton, *Nucleic Acids Res.* **2007**, *35*, 5182; e) B. Lebleu, H. M. Moulton, R. Abes, G. D. Ivanova, S. Abes, D. A. Stein, P. L. Iversen, A. A. Arzumanov, M. J. Gait, *Adv. Drug Delivery Rev.* **2008**, *60*, 517; f) J. M. Wolfe, C. M. Fadzen, Z.-N. Choo, R. L. Holden, M. Yao, G. J. Hanson, B. L. Pentelute, *ACS Cent. Sci.* **2018**, *4*, 512; g) J. M. Wolfe, C. M. Fadzen, R. L. Holden, M. Yao, G. J. Hanson, B. L. Pentelute, *Angew. Chem., Int. Ed.* **2018**, *57*, 4756.
- [12] P. A. Morcos, Y. Li, S. Jiang, *BioTechniques* **2008**, *45*, 613.
- [13] T. K. Warren, A. C. Shurtleff, S. Bavari, *Antiviral Res.* **2012**, *94*, 80.
- [14] a) C. Betts, A. F. Saleh, A. A. Arzumanov, S. M. Hammond, C. Godfrey, T. Coursindel, M. J. Gait, M. J. Wood, *Mol. Ther. – Nucleic Acids* **2012**, *1*, e38; b) C. A. Betts, A. F. Saleh, C. A. Carr, S. M. Hammond, A. M. Coenen-Stass, C. Godfrey, G. McClorey, M. A. Varela, T. C. Roberts, K. Clarke, M. J. Gait, M. J. Wood, *Sci. Rep.* **2015**, *5*, 8986; c) A. M. Blain, E. Grealley, G. McClorey, R. Manzano, C. A. Betts, C. Godfrey, L. O'Donovan, T. Coursindel, M. J. Gait, M. J. Wood, G. A. MacGowan, V. W. Straub, *PLoS One* **2018**, *13*, e0198897; d) C. A. Betts, G. McClorey, R. Healicon, S. M. Hammond, R. Manzano, S. Muses, V. Ball, C. Godfrey, T. M. Merritt, T. van Westering, L. O'Donovan, K. E. Wells, M. J. Gait, D. J. Wells, D. Tyler, M. J. Wood, *Hum. Mol. Genet.* **2019**, *28*, 396; e) S. M. Hammond, G. Hazell, F. Shabanpoor, A. F. Saleh, M. Bowerman, J. N. Sleight, K. E. Meijboom, H. Zhou, F. Muntoni, K. Talbot, M. J. Gait, M. J. Wood, *Proc. Natl. Acad. Sci. USA* **2016**, *113*, 10962.
- [15] a) E. Vivès, P. Brodin, B. Lebleu, *J. Biol. Chem.* **1997**, *272*, 16010; b) H. Brooks, B. Lebleu, E. Vivès, *Adv. Drug Delivery Rev.* **2005**, *57*, 559; c) A. Mishra, G. H. Lai, N. W. Schmidt, V. Z. Sun, A. R. Rodriguez, R. Tong, L. Tang, J. Cheng, T. J. Deming, D. T. Kamei, G. C. L. Wong, *Proc. Natl. Acad. Sci. USA* **2011**, *108*, 16883; d) G. Lättig-Tünnemann, M. Prinz, D. Hoffmann, J. Behlke, C. Palm-Apergi, I. Morano, H. D. Herce, M. C. Cardoso, *Nat. Commun.* **2011**, *2*, 453; e) H. D. Herce, A. E. Garcia, M. C. Cardoso, *J. Am. Chem. Soc.* **2014**, *136*, 17459.
- [16] a) O. Boussif, Lezoualc, F. h, M. A. Zanta, M. D. Mergny, D. Scherman, B. Demeneix, J. P. Behr, *Proc. Natl. Acad. Sci. USA* **1995**, *92*, 7297; b) S. H. Pun, N. C. Bellocq, A. Liu, G. Jensen, T. Machemer, E. Quijano, T. Schluelp, S. Wen, H. Engler, J. Heidel, M. E. Davis, *Bioconjugate Chem.* **2004**, *15*, 831; c) X.-L. Wang, R. Jensen, Z.-R. Lu, *J. Controlled Release* **2007**, *120*, 250; d) V. Russ, M. Günther, A. Halama, M. Ogris, E. Wagner, *J. Controlled Release* **2008**, *132*, 131; e) K. Miyata, M. Oba, M. Nakanishi, S. Fukushima, Y. Yamasaki, H. Koyama, N. Nishiyama, K. Kataoka, *J. Am. Chem. Soc.* **2008**, *130*, 16287; f) C. Lin, C.-J. Blaauboer, M. M. Timoneda, M. C. Lok, M. van Steenberg, W. E. Hennink, Z. Zhong, J. Feijen, J. F. J. Engbersen, *J. Controlled Release* **2008**, *126*, 166; g) H. Wei, J. A. Pahang, S. H. Pun, *Biomacromolecules* **2013**, *14*, 275.
- [17] a) J.-P. Behr, *Chimia Int. J. Chem.* **1997**, *51*, 34; b) H. Uchida, K. Miyata, M. Oba, T. Ishii, T. Suma, K. Itaka, N. Nishiyama, K. Kataoka, *J. Am. Chem. Soc.* **2011**, *133*, 15524; c) H. Uchida, K. Itaka, T. Nomoto, T. Ishii, T. Suma, M. Ikegami, K. Miyata, M. Oba, N. Nishiyama, K. Kataoka, *J. Am. Chem. Soc.* **2014**, *136*, 12396; d) U. Lächelt, P. Kos, F. M. Mickler, A. Herrmann, E. E. Salcher, W. Rödl, N. Badgular, C. Bräuchle, E. Wagner, *Nanomedicine* **2014**, *10*, 35; e) A. Jarzebińska, T. Pasewald, J. Lambrecht, O. Mykhaylyk, L. Kümmerling, P. Beck, G. Hasenpusch, C. Rudolph, C. Plank, C. Dohmen, *Angew. Chem., Int. Ed.* **2016**, *55*, 9591; f) L. M. P. Vermeulen, S. C. De Smedt, K. Remaut, K. Braeckmans, *Eur. J. Pharm. Biopharm.* **2018**, *129*, 184.
- [18] a) D. Schaffert, N. Badgular, E. Wagner, *Org. Lett.* **2011**, *13*, 1586; b) D. Schaffert, C. Troiber, E. E. Salcher, T. Fröhlich, I. Martin, N. Badgular, C. Dohmen, D. Edinger, R. Kläger, G. Maiwald, K. Farkasova, S. Seeber, K. Jahn-Hofmann, P. Hadwiger, E. Wagner, *Angew. Chem., Int. Ed. Engl.* **2011**, *50*, 8986.
- [19] N. J. Agard, J. A. Prescher, C. R. Bertozzi, *J. Am. Chem. Soc.* **2004**, *126*, 15046.
- [20] S. H. Kang, M. J. Cho, R. Kole, *Biochemistry* **1998**, *37*, 6235.
- [21] P. Kos, U. Lächelt, A. Herrmann, F. M. Mickler, M. Döblinger, D. He, A. Krhac Levacic, S. Morys, C. Bräuchle, E. Wagner, *Nanoscale* **2015**, *7*, 5350.
- [22] L. Beckert, L. Kostka, E. Kessel, A. Krhac Levacic, H. Kostkova, T. Etrych, U. Lächelt, E. Wagner, *Eur. J. Pharm. Biopharm.* **2016**, *105*, 85.
- [23] C. Scholz, P. Kos, E. Wagner, *Bioconjugate Chem.* **2014**, *25*, 251.
- [24] D. He, K. Müller, A. Krhac Levacic, P. Kos, U. Lächelt, E. Wagner, *Bioconjugate Chem.* **2016**, *27*, 647.
- [25] a) C. Troiber, D. Edinger, P. Kos, L. Schreiner, R. Kläger, A. Herrmann, E. Wagner, *Biomaterials* **2013**, *34*, 1624; b) P. M. Klein, S. Reinhard, D. J. Lee, K. Müller, D. Ponader, L. Hartmann, E. Wagner, *Nanoscale* **2016**, *8*, 18098.
- [26] a) G. Creusat, G. Zuber, *ChemBioChem* **2008**, *9*, 2787; b) G. Creusat, A.-S. Rinaldi, E. Weiss, R. Elbaghdadi, J.-S. Remy, R. Mulherkar, G. Zuber, *Bioconjugate Chem.* **2010**, *21*, 994; c) A. Ewe, S. Przybylski, J. Burkhardt, A. Janke, D. Appelhans, A. Aigner, *J. Controlled Release* **2016**, *230*, 13.
- [27] P. M. Klein, S. Kern, D. J. Lee, J. Schmaus, M. Höhn, J. Gorges, U. Kazmaier, E. Wagner, *Biomaterials* **2018**, *178*, 630.
- [28] a) C. S. Rocha, K. E. Lundin, M. A. Behlke, R. Zain, S. El Andaloussi, C. I. Smith, *Nucleic Acid Ther.* **2016**, *26*, 381; b) O. Saher, C. S. J. Rocha, E. M. Zaghoul, O. P. B. Wiklander, S. Zamolo, M. Heitz, K. Ezzat, D. Gupta, J. L. Raymond, R. Zain, F. Hollfelder, T. Darbe, K. E. Lundin, S. El Andaloussi, C. I. E. Smith, *Eur. J. Pharm. Biopharm.* **2018**, *132*, 29.
- [29] J. E. Summerton, *Ann. N. Y. Acad. Sci.* **2005**, *1058*, 62.
- [30] a) D. Magde, E. Elson, W. W. Webb, *Phys. Rev. Lett.* **1972**, *29*, 705; b) E. L. Elson, D. Magde, *Biopolymers* **1974**, *13*, 1; c) S. Ivanchenko, D. C. Lamb, in *Supramolecular Structure and Function 10* (Eds: J. Brnjas-Kraljević, G. Pifat-Mrzljak), Springer, Dordrecht, Netherlands **2011**, p. 1.
- [31] K. Ezzat, Y. Aoki, T. Koo, G. McClorey, L. Benner, A. Coenen-Stass, L. O'Donovan, T. Lehto, A. Garcia-Guerra, J. Nordin, A. F. Saleh, M. Behlke, J. Morris, A. Goyenvalle, B. Dugovic, C. Leumann, S. Gordon, M. J. Gait, S. El-Andaloussi, M. J. A. Wood, *Nano Lett.* **2015**, *15*, 4364.
- [32] a) T. Fröhlich, D. Edinger, R. Kläger, C. Troiber, E. Salcher, N. Badgular, I. Martin, D. Schaffert, A. Cengizeroglu, P. Hadwiger, H. P. Vornlocher, E. Wagner, *J. Controlled Release* **2012**, *160*, 532; b) S. Reinhard, W. Zhang, E. Wagner, *ChemMedChem* **2017**, *12*, 1464.
- [33] a) C. Plank, B. Oberhauser, K. Mechtler, C. Koch, E. Wagner, *J. Biol. Chem.* **1994**, *269*, 12918; b) L. M. P. Vermeulen, T. Brans, S. K. Samal, P. Dubruel, J. Demeester, S. C. De Smedt, K. Remaut, K. Braeckmans, *ACS Nano* **2018**, *12*, 2332.
- [34] S. Miyatake, Y. Mizobe, M. K. Tsoumpra, K. R. Q. Lim, Y. Hara, F. Shabanpoor, T. Yokota, S. i. Takeda, Y. Aoki, *Mol. Ther. – Nucleic Acids* **2019**, *14*, 520.
- [35] E. Araki, K. Nakamura, K. Nakao, S. Kameya, O. Kobayashi, I. Nonaka, T. Kobayashi, M. Katsuki, *Biochem. Biophys. Res. Commun.* **1997**, *238*, 492.
- [36] Y. Aoki, T. Yokota, T. Nagata, A. Nakamura, J. Tanihata, T. Saito, S. M. R. Duguez, K. Nagaraju, E. P. Hoffman, T. Partridge, S. i. Takeda, *Proc. Natl. Acad. Sci. USA* **2012**, *109*, 13763.